The Meteoritical Society

Meteoritics & Planetary Science 43, Nr 9, 1487–1496 (2008)
Abstract available online at http://meteoritics.org

Micro-Raman spectroscopic study of fine-grained, shock-metamorphosed rock fragments from the Australasian microtektite layer

Billy P. GLASS[1*] and Marc FRIES[2]

[1]Department of Geological Sciences, University of Delaware, Newark, Delaware 19716, USA
[2]Geophysical Laboratory, Carnegie Institution of Washington, 5251 Broad Branch Rd., NW, Washington, D.C. 20015, USA
[*]Corresponding author. E-mail:bglass@udel.edu

(Received 19 September 2007; revision accepted 15 April 2008)

Abstract–Shock-metamorphosed rock fragments have been found in the Australasian microtektite layer from the South China Sea. Previous X-ray diffraction (XRD) studies indicate that the most abundant crystalline phases in the rock fragments are coesite, quartz, and a 10 Å phase (mica/clay?). In addition, the presence of numerous other phases was suggested by scanning electron microscopy (SEM) and energy-dispersive X-ray (EDX) analysis. In the present research, ten of the rock fragments, which had previously been studied using SEM/EDX, were studied by micro-Raman spectroscopy. The presence of K-feldspar, plagioclase, rutile, ilmenite, titanite, magnetite, calcite, and dolomite were confirmed. In addition, the high-pressure TiO_2 polymorph with an α-PbO_2 structure (i.e., TiO_2II) was found in several rock fragments. Two grains previously thought to have been zircon, based on their compositions, were found to have Raman spectra that do not match the Raman spectra of zircon, reidite, or any of the possible decomposition products of zircon or their high-pressure polymorphs. We speculate that the $ZrSiO_4$ phase might be a previously unknown high-pressure polymorph of zircon or one of its decomposition products (i.e., ZrO_2 or SiO_2). The presence of coesite and TiO_2 II, and partial melting and vesiculation suggest that the rock fragments containing the unknown $ZrSiO_4$ phase must have experienced shock pressures between 45 and 60 GPa. We conclude that micro-Raman spectroscopy, in combination with XRD and SEM/EDX, is a powerful tool for the study of small, fine-grained impact ejecta.

INTRODUCTION

Australasian tektites have been found in southern China, Indochina, the Philippines, Malaysia, Indonesia, and Australia. Microtektites belonging to this strewn field have been found throughout much of the Indian Ocean, the western equatorial Pacific Ocean, and the South China, Philippine, Celebes, and Sulu seas (Glass and Koeberl 2006; and references therein). Radiometric dating ($^{40}Ar/^{39}Ar$) indicates that the Australasian tektites were formed ~0.8 Ma ago (Izett and Obradovich 1992; Kunz et al. 1995; Yamei et al. 2000). Paleomagnetic studies of cores containing the Australasian microtektite layer indicate that the microtektites fell ~14 ka before the Brunhes-Matuyama reversal boundary (Burns 1989; Schneider et al. 1992; Lee and Wei 2000) or ~0.8 Ma ago. Geochemical studies suggest that the source deposit for the Australasian tektites was sediment or sedimentary rock, possibly a graywacke (e.g., Taylor and Kaye 1969). The size, shape, and mineral assemblage of inclusions recovered from Muong Nong-type Australasian tektites also indicate a sedimentary source rock and suggest that it was fine grained (Glass and Barlow 1979). Wasson and Heins (1993) suggested that the source deposit might have been dry loess.

The location of the source crater for the Australasian tektites is unknown, but most tektite investigators suggest that it is somewhere in the Indochina region (e.g., Stauffer 1978; Ford 1988; Schnetzler 1992; Koeberl 1994; Ma et al. 2004). Geographic variation in the microtektite abundances is consistent with a source crater in the Indochina area (Glass and Pizzuto 1994; Lee and Wei 2000; Glass and Koeberl 2006). The abundance of microtektites increases toward the Indochina region with the highest abundances being found in the South China Sea (Glass and Koeberl 2006) (Fig. 1). The highest abundances of unmelted impact ejecta are also found in the South China Sea (Glass and Koeberl 2006).

Glass and Koeberl (2006) did a petrographic and geochemical study of microtektites and shocked-rock fragments in cores from three sites in the South China Sea: Core SONNE-95-17957-2 (Sarnthein et al. 1994) and at Ocean Drilling Program (ODP) Site 1143 in the central South

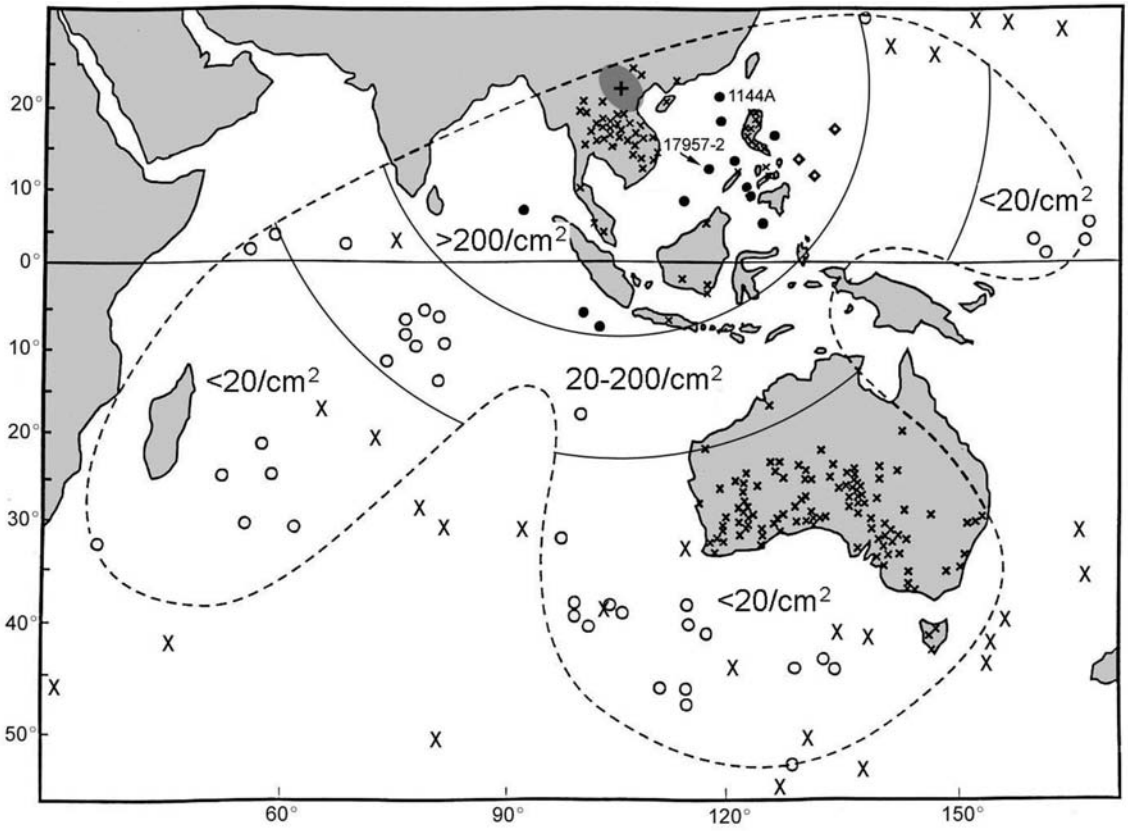

Fig. 1. Map of the Australasian tektite/microtektite strewn field. Tektite locations on land indicated schematically with small Xs. Locations of deep-sea sediment cores containing the Australasian microtektite layer without associated unmelted ejecta indicated by open circles. Locations of deep-sea sediments containing the Australasian microtektite layer with associated unmelted ejecta (shocked rock and mineral grains, coesite) indicated with solid circles. The locations of the two cores from which shocked-rock fragments used in this study were recovered (ODP Hole 1144A and 17957-2) are labeled. Locations (just east of the Philippines) of cores containing shocked quartz and coesite, but not microtektites, are indicated by diamond-shaped symbols. The proposed location of the source crater is within the shaded area (with a plus sign in the center) in the northern Indochina area (see Glass and Koeberl 2006). The number of estimated microtektites per cm^2 at each site varies from <20 farthest away from the proposed crater site to >200 closer to the proposed crater site. Cores with the highest abundance of microtektites are also the cores that contain shocked mineral grains, and in some cases shocked-rock fragments. The greatest abundance of microtektites and shocked mineral grains and rock fragments is at Ocean Drilling Program Hole 1144A in the northern South China Sea. Modified after Fig. 1 in Glass and Koeberl (2006).

China Sea and ODP Site 1144 in the northern South China Sea. They found the highest abundances of microtektites and unmelted ejecta at ODP Site 1144. The unmelted ejecta were composed of white opaque grains and fine-grained (grain size generally <50 μm) rock fragments (Fig. 2) up to ~600 μm in maximum dimension. X-ray diffraction (XRD) studies showed that the white opaque grains consist of mixtures of quartz, coesite, and, sometimes, stishovite and indicate that the crystalline phases in the rock fragments are mostly coesite, quartz, and a 10 Å phase (mica/clay?) (Glass and Koeberl 2006).

Scanning electron microscope (SEM) and energy dispersive X-ray (EDX) analyses show that the larger grains in the rock fragments have compositions indicating the presence of silica (probably quartz and coesite, as indicated by XRD studies) and feldspar (mostly K-feldspar, but with some plagioclase). The trace minerals had compositions suggesting the presence of: rutile, garnet, ilmenite, zircon, titanite, and iron oxide phases, in approximate decreasing order of abundance. In addition, one grain each with the composition of barite, apatite, and an Al_2SiO_5 phase were found (Glass and Koeberl 2006). Also several Ca-rich and Ca- and Mg-rich grains where found that were thought to be calcite and dolomite, respectively. The bulk major and trace element compositions of the grains indicate that their compositions are similar to the compositions of the Australasian tektites and microtektites, suggesting that they may be fragments of the source rocks which were melted to produce the tektites and microtektites (Glass and Koeberl 2006).

The purpose of this research was to confirm (or not) by Raman spectroscopy the phase identifications based on major element compositions and to search for high-pressure polymorphs of the trace minerals.

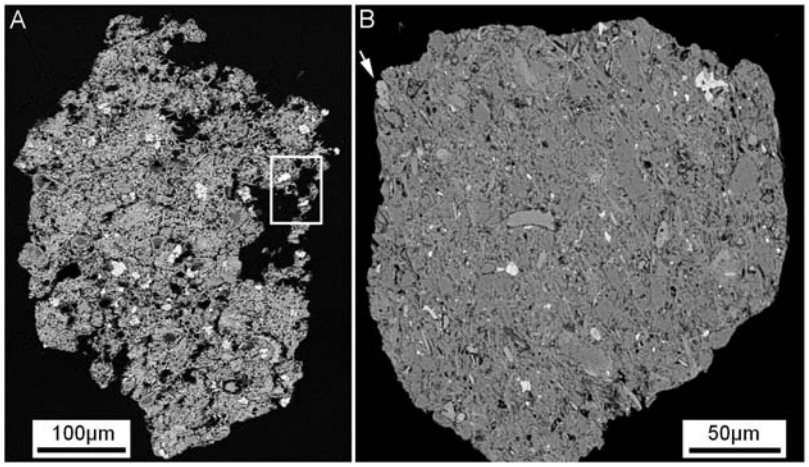

Fig. 2. Backscattered electron images of two shocked-rock fragments from the Australasian microtektite layer in the South China Sea. A. Sample 885-1 from ODP Hole 1144A in the northern South China Sea. It is heavily shocked as indicated by partial melting, vesiculation, and the presence of TiO_2II, a high-pressure polymorph of rutile. The area in the white box is enlarged in Fig. 10. It shows the vesiculation, the TiO_2II phase, and an unidentified Zr silicate phase (perhaps a previously unrecognized high-pressure polymorph of zircon) at higher magnification. B. Sample 889-6 from Core 17957-2 from the central South China Sea. X-ray diffraction data indicate that the major crystalline phases in this rock fragment are coesite and a 10 Å phase (mica?). A light grey, Ca-rich (as determined by energy dispersive X-ray data) phase in the upper left corner was identified as a carbonate by its Raman spectrum.

METHODS

We removed, by polishing, as much of the carbon coating as we could, without removing the grains that had previously been studied by SEM/EDX, from two polished grain mounts containing shocked rock fragments. One slide contained ten rock fragments from ODP Site 1144 (lat 20.05° N, long 117.42° E; Wang et al. 2000) and the other contained eleven rock fragments from Core SONNE-95-17957-2 (lat 10.90° N., long 115.31° E; Sarnthein et al. 1994). Based on previously obtained back-scattered electron images and major element compositional data (obtained by EDX analysis), six rock fragments from ODP Site 1144 and four rock fragments from Core SONNE-95-17957-2 (hereafter referred to as Core 17957-2) were selected for Raman spectroscopy. XRD patterns had been obtained for the rock fragments from Core 17957-2 prior to mounting them for preparation of the polished grain mounts. The XRD patterns of the four rock fragments from Core 17957-2, investigated in this study, indicate that the most abundant crystalline phase is coesite. A 10 Å phase was present in all four rock fragments, but quartz was observed in only one of the rock fragments.

Raman spectroscopy was performed with a WITec SNOM microscope customized to include Raman spectroscopic imaging using a 532 nm wavelength, frequency-doubled Nd:YAG laser. Selected samples were analyzed using a 100× objective lens generating a calculated spot size of 360 nm diameter. Laser power was restricted to 0.055 mW as measured at the focal plane, for a calculated power density of 420 kW/cm^2 with an integration time that varied between 1 and 175 seconds. These parameters were selected for individual measurements based on the desired quality of the resulting spectrum, sample fluorescence intensity, and Raman signal strength. Collected sample spectra were compared against spectra from standard materials, primarily from the RRUFF database project (Downs 2006).

Raman spectra produced in this study appear to be of relatively unimpressive quality out of necessity, but in fact these spectra are an improvement over those which could be obtained with many commercially available systems. Since the target materials were expected to contain metastable phases, spectra were collected with an emphasis on obtaining usable spectra while maintaining a bare minimum of total laser energy deposited on the target. Additionally, the sample materials are shocked and largely composed of very fine-grained material with a reduced content of crystalline material, both of which tend to produce spectra with a strong fluorescence component and weak Raman signal. These parameters necessitated the use of a very small spot size to preferentially select small crystalline regions and a small confocal pinhole to suppress fluorescence which had the side effect of attenuating the signal intensity, in addition to the reduced laser power setting selected to prevent damage to metastable phases. The resulting Raman spectra featured low signal to noise values as a consequence. Where possible, multiple spectra were added to improve the resulting spectra, but in general the collection of spectra was governed by the principle of obtaining sufficient quality to identify a phase while avoiding damage to the sample.

RESULTS

Most of the grains were highly fluorescent, probably due to shock metamorphism, and did not give spectra with any

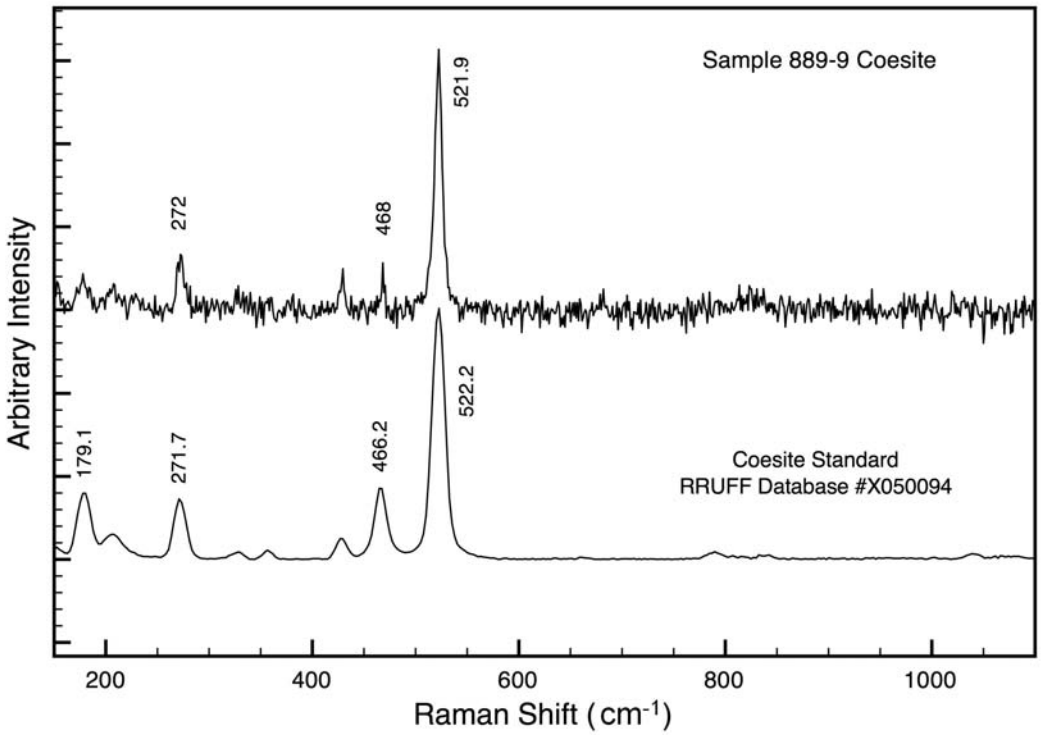

Fig. 3. Raman spectrum of coesite. Although coesite was a major phase in all the rock fragments that were X-rayed, it was difficult to identify by Raman spectroscopy, even though the SiO_2-rich grains had already been identified by energy dispersive X-ray analysis. All Raman spectral standards are from the RRUFF Raman spectral database unless otherwise noted (http://rruff.geo.arizona.edu/rruff).

identifiable peaks. Some samples showed hints of a glassy phase (diaplectic glass?), but the low power settings used to examine the samples did not give convincing spectra.

XRD patterns had indicated that the major crystalline phases in the rock fragments are coesite and quartz. We obtained spectra for numerous grains in several rock fragments that had previously been identified as quartz or coesite based on their SiO_2 compositions determined by SEM/EDX. Only a couple of these grains produced spectra that are consistent with coesite (Fig. 3) and none of the silica grains yielded a quartz spectrum.

Although XRD did not indicate the presence of feldspar in any of the rock fragments, numerous grains in the rock fragments were found to have major oxide compositions consistent with K-feldspar and plagioclase. We attempted to get Raman spectra for many of these grains, in several different rock fragments, but we were only successful in obtaining spectra from a few grains that are consistent with the presence of plagioclase and orthoclase (Fig. 4); but the spectra are of poor quality.

XRD patterns indicated that a 10 Å phase (probably a phyllosilicate) was present in most of the rock fragments. We were not able to identify the 10 Å phase using SEM/EDX, but we did find some regions with a platy phase that might be a phyllosilicate. We tried to obtain Raman spectra for several of these platy grains without success, but finally were able to obtain a poor quality Raman spectrum for one of these grains that is consistent with a mica, probably muscovite.

We identified a few grains in a couple of the rock fragments that could be carbonate minerals (i.e., calcite and dolomite) based on their major oxide compositions. We obtained spectra consistent with carbonate (Fig. 5) for a couple of these grains and thus confirmed the presence of carbonate fragments in some of the rock fragments. We also confirmed the presence of titanite, apatite, and rutile (Fig. 6) and garnet (Fig. 7). The best match for the garnet appears to be spessartine. On the other hand, we had previously identified several grains as possibly being garnet based on their major oxide compositions and none were rich in Mn; most were Ca or Fe rich. We had identified several Fe-rich grains by SEM/EDX. One of these grains was identified as magnetite by its Raman spectrum (Fig. 6). We did not know that magnetite was present in these rock fragments prior to the Raman study. We also found two other phases that we had not known were present in these samples prior to this study: a high-pressure polymorph of rutile (TiO_2II), and an unknown phase with a Zr silicate composition.

Raman spectra of several of the grains, previously identified as possibly rutile based on their compositions, indicate that the grains are mostly the rutile polymorph with an α-PbO_2 structure (also known as TiO_2II) (Fig. 8). In addition, we obtained Raman spectra for two grains (one each

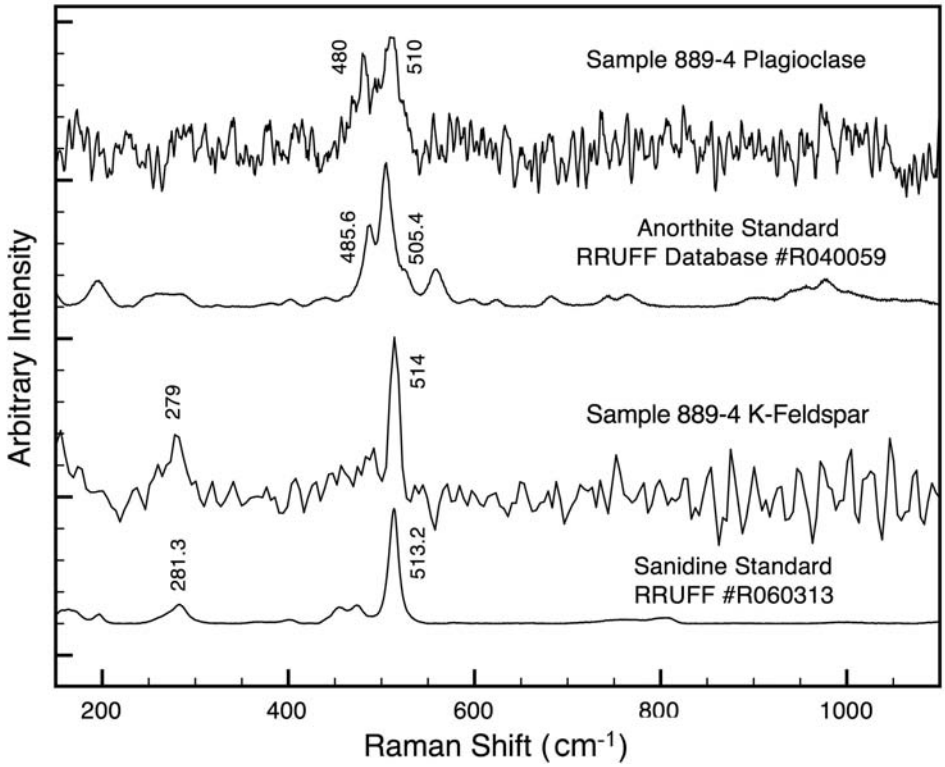

Fig. 4. Raman spectra of grains previously identified as plagioclase and K-feldspar based on their major oxide compositions. The feldspar spectra are of poor quality because of destruction of most of the crystalline structure due to shock metamorphism; however, the spectra, along with the major oxide compositions of the grains, are good enough to confirm the identification of these phases.

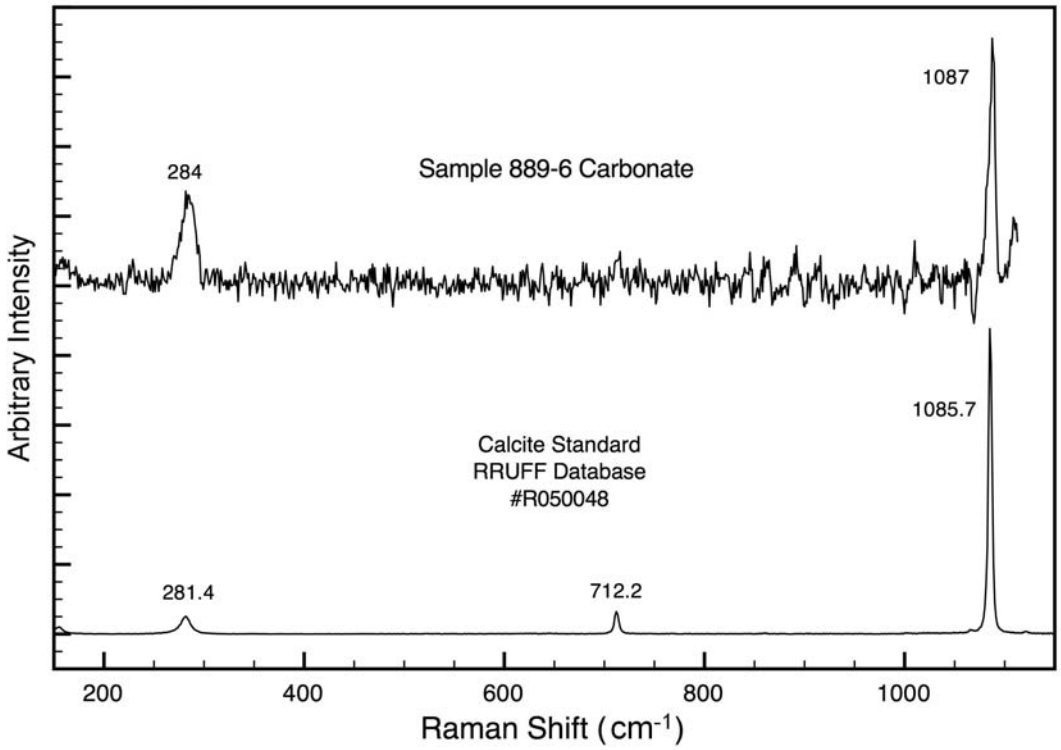

Fig. 5. Raman spectrum of a Ca-rich grain previously identified as possibly calcite. The Raman spectrum is consistent with this identification.

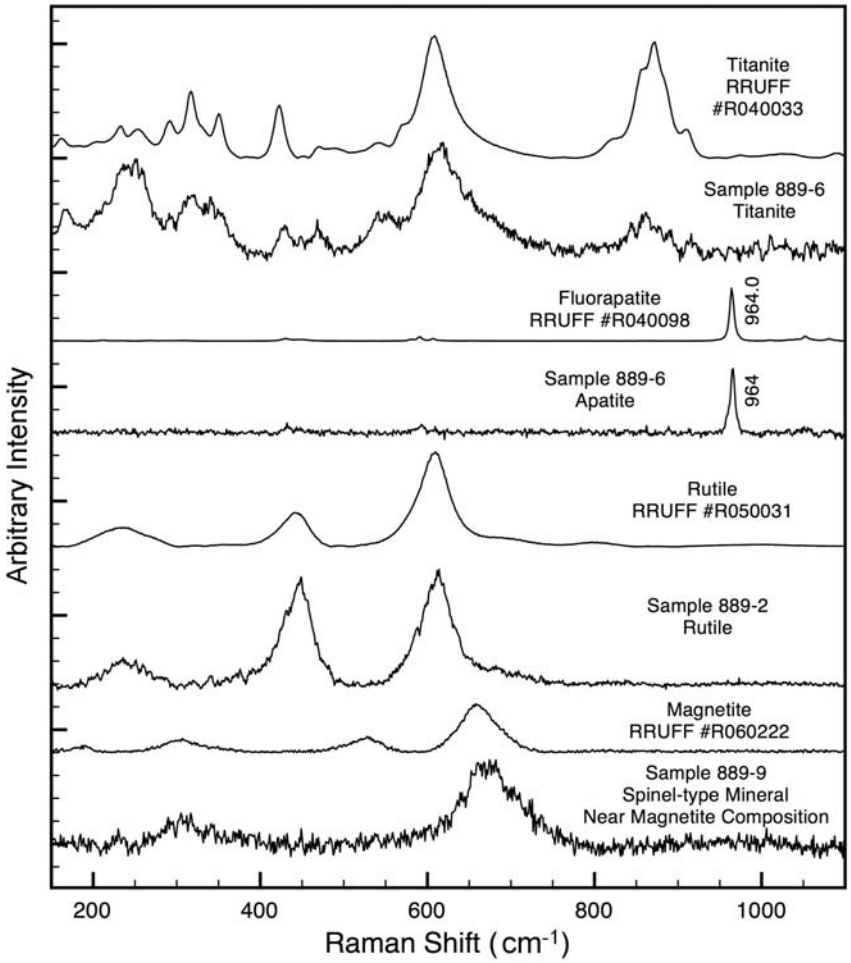

Fig. 6. Raman spectra of grains identified as titanite, apatite, rutile, and magnetite. These identifications are consistent with their major oxide compositions.

in two different rock fragments) previously identified as zircon based on their $ZrSiO_4$ compositions as determined by EDX analysis. These spectra did not match those of zircon or reidite or any possible breakdown phases of zircon, such as baddeleyite (or any of its polymorphs) or any of the silica polymorphs (e.g., quartz, stishovite) that we know (Fig. 9). This phase may be a new, previously unrecognized, high-pressure polymorph of zircon or of one of its decomposition products (i.e., ZrO_2 or SiO_2).

DISCUSSION

Micro-Raman spectroscopy, in combination with XRD and SEM/EDX, provides a powerful tool for the study of fine-grained impact ejecta. The present research involved the study of small (<600 μm), fine-grained, shock-metamorphosed, rock fragments recovered from the Australasian microtektite layer. Previous XRD studies of the rock fragments indicated that the most abundant crystalline phases are coesite and quartz and a 10 Å phase, while SEM/EDX studies suggested the presence of K-feldspar and plagioclase as well as a number of minor phases including rutile, garnet, ilmenite, zircon, titanite, iron oxide phases, apatite, barite, and possibly calcite and dolomite, in approximate decreasing order of abundance (Glass and Koeberl 2006). In the present research, we studied these rock fragments using micro-Raman spectrocopy. We used backscattered electron images of the rock fragments along with compositional data for individual grains in the rock fragments to locate grains of interest for micro-Raman spectroscopy. In spite of flourescence problems, we were able to confirm the presence of coesite, K-feldspar, plagioclase and many of the minor phases previously identified by XRD and SEM/EDX. In addition, we discovered that a number of the rock fragments contain the high-pressure polymorph of rutile with an α-PbO_2 structure (TiO_2II) and possibly an unknown high-pressure polymorph of zircon or one of its decomposition products. Thus, each of the methods provided useful information about the rock fragments, but none of the methods by themselves told the complete story.

The poor quality of the spectra in this study was probably due to the fine grain size and fluorescene due to shock

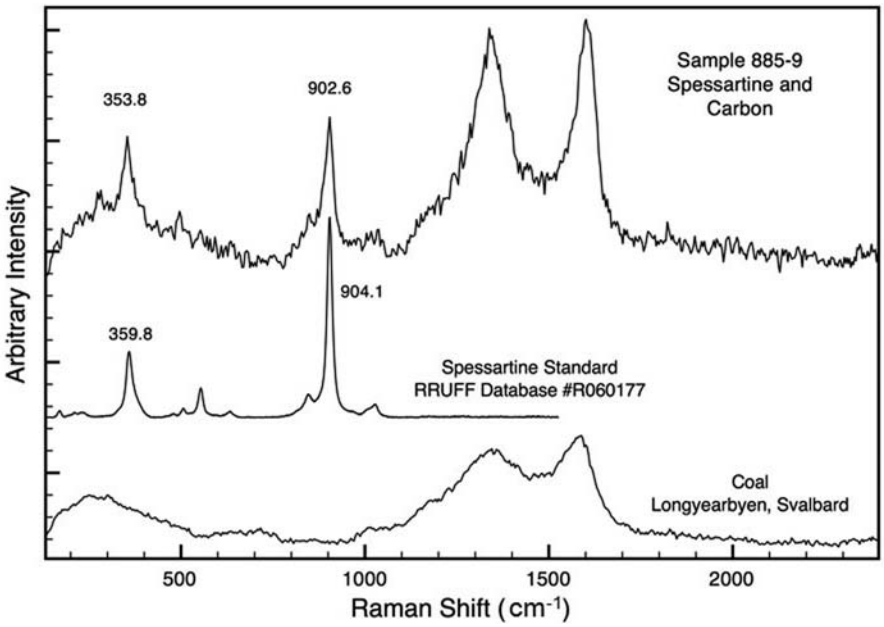

Fig. 7. Raman spectrum of a mixture of spessartine and carbon. The carbon is probably from the carbon coating, which may not have been removed completely from this grain. Standard spectrum of spessartine is from the RRUFF Raman spectra database (http://rruff.geo.arizona.edu/rruff), and the coal sample was collected from a mining operation in Longyearbyen, Svalbard.

metamorphism. The WITec sytem used in this study is not the best instrument for spectral quality, but it was a trade-off to get the very small spot size required for this study and for fluorescence suppression. Some of the grains of interest, including the $ZrSiO_4$ grains, where <10 μm in maximum dimension. Longer acquisition times did not seem to improve the quality of the spectra.

Based on grain size and shape of the grains and the mineral assemblage present (including coesite) in the shocked-rock fragments from the Australasian microtektite layer, Glass and Koeberl (2006) concluded that the source rock was a fine-grained sedimentary rock or sediments that were shock lithified. The confirmation of angular to rounded grains of calcite and dolomite in the rock fragments supports the conclusion that the source rock was sedimentary in nature.

The discovery of a high-pressure polymorph of rutile (TiO_2II) in rock fragments recovered from the Australasian microtektite layer provides further evidence that these rock fragments have been shock metamorphosed. The rock fragments containing the $ZrSiO_4$ grains with unknown Raman spectra also contain coesite, the TiO_2II phase, and evidence of partial melting and vesiculation (Fig. 10). Coesite is known to form at shock pressures between 30 and 60 GPa (Stöffler and Langenhorst 1994); the TiO_2II phase has been formed by shock experiments at pressures of 33 and 75 GPa (McQueen et al. 1967; Linde and DeCarli 1969); and partial melting of silicate rock begins at ~45–50 GPa (French 1998). Thus, the rock fragments containing the $ZrSiO_4$ grains with unknown Raman spectra must have experienced shock pressures in the range between 45 and 60 GPa. This is within the range of shock pressure required to produce reidite. Thus, it is not clear why the zircons were not transformed to reidite and the presence of $ZrSiO_4$ grains with unknown Raman spectra remains a mystery.

It has been suggested that the spectra obtained for the Zr silicate grains may not be Raman spectra, but instead may be the results of luminescence effects, possibly due to the presence of trace amounts of rare earth elements like Er^{3+} or Ho^{3+} in the Zr silicate grains. Such an effect can be ruled out by using a different laser excitation source. Unfortunately, this could not be done. After studying the grains using Raman spectroscopy, the samples were re-coated and the grains which produced the unknown spectra were analyzed again using SEM/EDX to confirm that these grains were in fact Zr silicate. After confirming that the grains are Zr silicate, the coating was removed by re-polishing so that the grains could be studied again using Raman spectroscopy; unfortunately, the Zr silicate grains were lost during re-polishing. Although we cannot check for luminescence effects using a different laser excitation source, we do not believe the spectra are due to luminescence effects for the reasons given below.

During our Raman spectroscopic study of the Zr silicate grains, we made a Raman spectral scan of one of the Zr silicate grains using the intensity of a Gaussian fit to the 779 cm^{-1} peak to image the unknown phase. There are changes in the relative intensities of two of the peaks (at ~730 and 779 cm^{-1}) of the unknown spectrum from one part of the grain to another. The changes in relative intensities of two peaks in the spectra are consistent with the behavior of Raman spectra, while this effect is not readily explained if it arises from luminescence. Changes in relative intensities of two peaks in a Raman spectrum can be caused by minor changes in

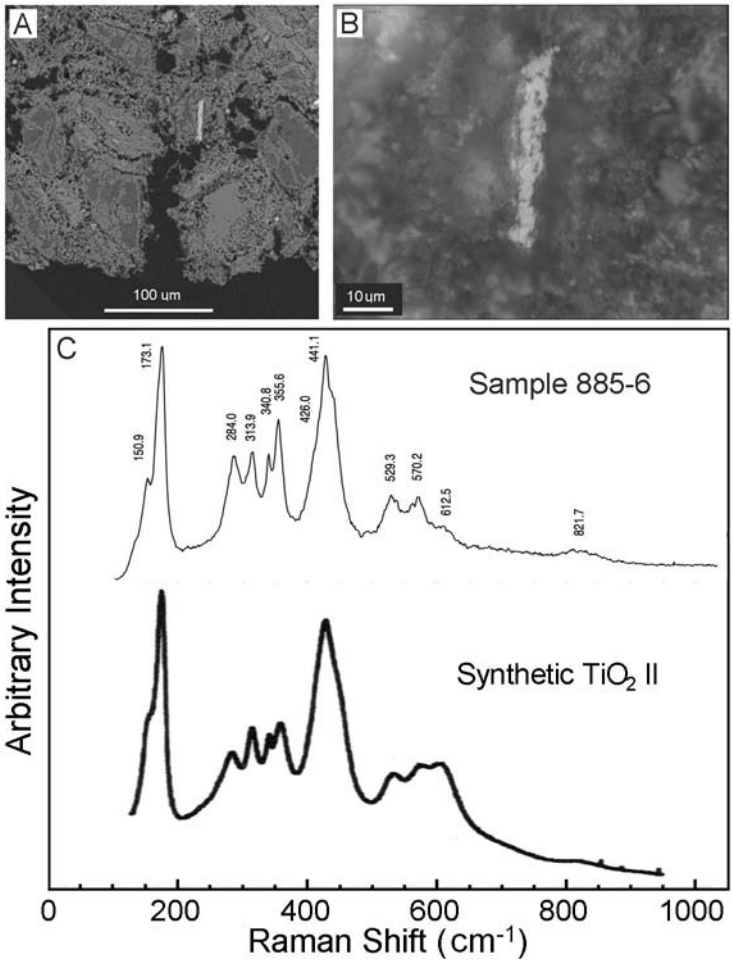

Fig. 8. A) Backscattered electron image of a shocked-rock fragment from the Australasian microtektite layer at ODP Hole 1144A in the northern South China Sea. The ~40 μm long bright grain just to the upper right of the center was identified as possibly rutile based on major oxide composition. B) Grain in A as seen in the microscope used for Raman spectroscopy. C) Raman spectrum (885-6) of the elongate bright grain in (A) and (B) compared with synthetic TiO_2II (from El Goresy et al. 2001). The match is very good.

crystalline orientation in a polycrystalline phase. In addition, the definition between the peaks and low intensity relative to the power of the excitation beam are more typical of a Raman spectrum than a luminescence spectrum which tends to have broader, more intense peaks.

As mentioned above, the peaks at ~730 and 779 cm^{-1} in the spectra produced during a scan of one of the Zr silicate grains exhibit changes in their relative intensities from one part of the grain to another. They tend to vary as opposing pairs; the 730 peak is more intense when the 779 peak is weaker and vice versa. In both this behavior and general spectral position, these peaks are comparable to SiO_4 tetrahedron symmetric and anti-symmetric stretch modes. The same modes appear in olivine at ~820 and ~850 cm^{-1}. Olivine also shares the peaks intensity variation traits with the unknown Zr silicate phase as well. When the symmetric peak is strong, the anti-symmetric peak is weak and vice versa. This is a function of the crystalline orientation to the excitation beam, and is also more typical of a Raman mode than a rare earth element luminescence event.

It is possible, as previously mentioned, that the unknown Raman spectra produced by the $ZrSiO_4$ grains could be an unknown high-pressure polymorph of one of the decomposition products and would thus be a ZrO_2 or SiO_2 phase. We do not believe this is the case, however. We obtained EDX spectra on both of these grains before and after studying them by Raman spectroscopy and all four spectra were similar to $ZrSiO_4$—i.e., there was no obvious evidence of ZrO_2- or SiO_2-rich regions within the grains. Also, if the variations in Raman peak intensity were due to variations in the volume of two phases, we would expect to see variations in the relative intensities of all peaks of the second phase, rather than just the balanced intensity variation between the two major peaks that is observed. Additionally, no evidence is seen for any silica phase in the Raman spectral imaging of the Zr silicate grain.

In a search of the latest version of the RRUFF Raman spectra database we found a triclinic mineral (umohoite) with a Raman spectrum very similar to the unknown Zr silicate spectrum. However, this mineral has the composition

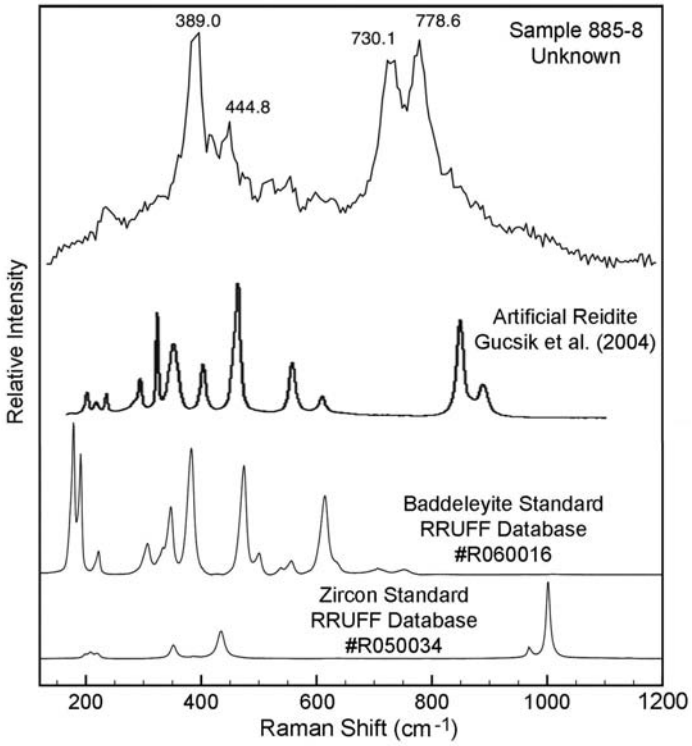

Fig. 9. Raman spectrum of a Zr silicate grain in a shocked-rock fragment from ODP Hole 1144A. The spectrum does not match that of zircon, baddeleyite, or reidite (or any of the high-pressure polymorphs of ZrO_2 that we know). It may be from a previously unknown high-pressure polymorph of zircon.

$(UO_2)MoO_4 + 4H_2O$ and thus could not be responsible for the unknown Zr silicate spectrum. However, the similarity between the Raman spectra suggests that these two phases have similar crystal structures.

CONCLUSION

In the present study, micro-Raman spectroscopy, in combination with SEM/EDX was used to confirm the presence of coesite, K-feldspar, plagioclase, rutile, garnet, titanite, apatite, calcite and dolomite in small (<700 μm), fine-grained, shock-metamorphosed, rock fragments recovered from the Australasian microtektite layer.

Confirmation of the presence of calcite and dolomite grains in the rock fragments supports the suggestion (Glass and Koeberl 2006) that the rock fragments are sedimentary in nature.

During the present study, we discovered the presence of a high-pressure polymorph of rutile with an α-PbO_2 structure called TiO_2II. The presence of the TiO_2II phase, along with evidence of partial melting of the silicate phases in the rock fragments, indicates that the rock fragments containing this phase probably experienced shock pressures in the range between 45 and 60 GPa.

We found that two grains with approximate $ZrSiO_4$ composition, which were originally thought to be zircons, produce unknown Raman spectra. We speculate that the spectra might be of an unknown high-pressure polymorph of zircon. The Raman spectrum of this phase is very similar to the Raman spectrum of umohoite.

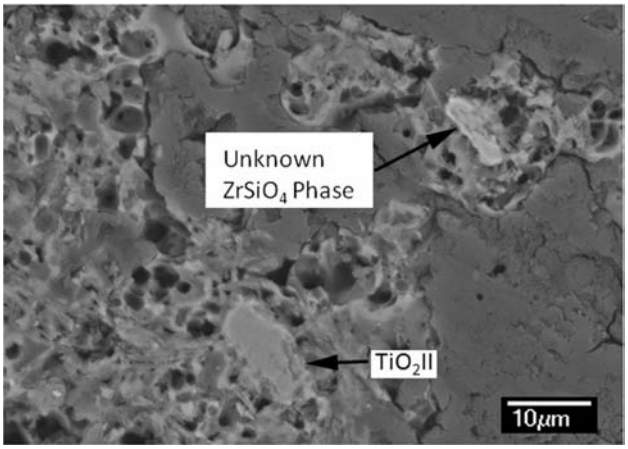

Fig. 10. A backscattered electron image of a portion of the grain shown in Fig. 2A showing a TiO_2II grain and the unknown $ZrSiO_4$ phase. It can be seen that these grains are in a rock fragment that is quite vesicular. The smoother, medium-grey region is epoxy.

We conclude that micro-Raman spectroscopy, in combination with XRD and SEM/EDX, is a powerful tool for investigating small samples of fine-grained, shock-metamorphosed impact ejecta.

Acknowledgments–We thank M. Sarnthein for help in

acquiring samples from Core SONNE-95-17957-2 and the Ocean Drilling Program for samples from ODP Hole 1144A. We thank Eugen Libowitzky and Ming Zhang for critical review of the paper and for helpful suggestions.

Editorial Handling—Dr. Christian Koeberl

REFERENCES

Burns C. A. 1989. Timing between a large impact and a geomagnetic reversal and the depth of NRM acquisition in deep-sea sediments. In *Geomagnetism and palaeomagnetism*, edited by Lowes F. J., Collinson, D.W.; Parry J. H., Runcorn S. K., Tozer D. C., and Soward A. Dordrecht: Kluwer Academic Publishers. pp. 253–261.

Downs R. T. 2006. The RRUFF Project: An integrated study of the chemistry, crystallography, Raman and infrared spectroscopy of minerals (abstract #O03–13). 19th General Meeting of the International Mineralogical Association. CD-ROM.

El Goresy A., Chen M., Gillet P., Dubrovinsky L., Graup G., and Ahuja R. 2001. A natural shock-induced dense polymorph of rutile with α-PbO_2 structure in the suevite from the Ries crater in Germany. *Earth and Planetary Science Letters* 192:485–495.

Ford R. J. 1988. An empirical model for the Australasian tektite field. *Australian Journal of Earth Sciences* 35:483–490.

French B. M. 1998. *Traces of catastrophe: A handbook of shock-metamorphic effects in terrestrial meteorite structures*. LPI Contribution 954. Houston: Lunar and Planetary Institute. 120 p.

Glass B. P. and Barlow R. A. 1979. Mineral inclusions in Muong Nong-type indochinites: Implications concerning parent material and process of formation. *Meteoritics* 14:55–67.

Glass B. P. and Koeberl C. 2006. Australasian microtektites and associated impact ejecta in the South China Sea and the Middle Pleistocene supereruption of Toba. *Meteoritics & Planetary Science* 41:305–326.

Glass B. P. and Pizzuto J. E. 1994. Geographic variation in Australasian microtektite concentrations: Implications concerning the location and size of the source crater. *Journal of Geophysical Research* 99:19,075–19,081.

Izett G. A. and Obradovich J. D. 1992. Laser-fusion $^{40}Ar/^{39}Ar$ ages of Australasian tektites (abstract). 23rd Lunar and Planetary Science Conference. pp. 593–594.

Koeberl C. 1994. Tektite origin by hypervelocity asteroidal or cometary impact: Target rocks, source craters, and mechanisms. In *Large impacts and planetary evolution*, edited by Dressler B. O., Grieve R. A. F., and Sharpton V. L. GSA Special Paper 293. Boulder, Colorado: Geological Society of America. pp. 133–151.

Kunz J., Bollinger K., Jesseberger E. K., and Storzer D. 1995. Ages of Australasian tektites (abstract). 26th Lunar and Planetary Science Conference. pp. 809–810.

Lee M. -Y. and Wei K. -Y. 2000. Australasian microtektites in the South China Sea and the West Philippine Sea: Implications for age, size, and location of the impact crater. *Meteoritics & Planetary Science* 35:1151–1155.

Linde R. K. and DeCarli P. S. 1969. Polymorphic behavior of titania under dynamic loading. *Journal of Chemical Physics* 50:319–325.

Ma P., Aggrey K., Tonzola C., Schnabel C., de Nicola P., Herzog G. F., Wasson J. T., Glass B. P., Brown L., Tera F., Middleton R., and Klein J. 2004. Beryllium-10 in Australasian tektites: Constraints on the location of the source crater. *Geochimica et Cosmochimica Acta* 68:3883–3896.

McQueen R. G., Jamieson J. C., and Marsh S. P. 1967.Shock-wave compression and X-ray studies of titanium dioxide. *Science* 155: 1401–1404.

Sarnthein M., Pflaumann U., Wang P., and Wong H. K., eds. 1994. Preliminary report on Sonne-95 cruise "Monitor monsoon" to the South China Sea. *Berichte Reports* 68, Kiel, Germany: Geologisch-Paläontologisches Institut, Universität Kiel. 225 p.

Schneider D. A., Kent D. V., and Mello G. A. 1992. A detailed chronology of the Australasian impact event, the Brunhes-Matuyama geomagnetic polarity reversal, and global climate change. *Earth and Planetary Science Letters* 111:395–405.

Schnetzler C. C. 1992. Mechanism of Muong Nong-type tektite formation and speculation on the source of the Australasian tektites. *Meteoritics* 27:154–165.

Stauffer P. H. 1978. Anatomy of the Australasian tektite strewnfield and the probable site of its source crater. 3rd Regional Conference on Geology and Mineral Resources of Southeast Asia. pp. 285–289.

Stöffler D. and Langenhorst F. 1994. Shock metamorphism of quartz in nature and experiment: I. Basic observations and theory. *Meteoritics* 29:155–181.

Taylor S. R. and Kaye M. 1969. Genetic significance of the chemical composition of tektites: A review. *Geochimica et Cosmochimica Acta* 33:1083–1100.

Wang P., Prell W. L., Blum P., et al. 2000. Proceedings, Ocean Drilling Program, Initial Reports, vol. 184. CD-ROM.

Wasson J. T. And Heins W. A. 1993. Tektites and climate. *Journal of Geophysical Research* 98:3043–3052.

Yamei H., Potts R., Baoylin Y., Zhengtang G., Deino A., Wei W., Clark J., Guangmao X., and Weiwen H. 2000. Mid-Pleistocene Acheulean-like stone technology of the Bose Basin, South China. *Science* 287:1622–1626.